

SOURCE LOCATION ALGORITHM FOR INFRASONIC MONITORING

Milton Garces,¹ Claus Hetzer,¹ Kent Lindquist,² and Douglas Drob³

University of Hawaii Manoa,¹ Lindquist Consulting,² and Naval Research Laboratory³

Sponsored by National Nuclear Security Administration
Office of Nonproliferation Research and Engineering
Office of Defense Nuclear Nonproliferation

Contract No. DE-FC04-98AL79801

ABSTRACT

Two large bolides have been recorded by International Monitoring System (IMS) infrasound stations in Hawaii and Alaska. On 25 August 2000 at 01:12:25 UTC, Department of Defense and Department of Energy satellites observed an object at 14.45 North and 106.13 West, with a total visible estimated energy of 1.4×10^{12} joules. This object, known as the Acapulco bolide, was observed by IMS stations in Hawaii, Alaska, Bolivia, Canada, and French Guiana, as well as by DLIAR in New Mexico. On 23 April 2001, at 06:12:35 UTC, satellites observed an object at an altitude of 28.5 km at 27.9 North and 133.89 West, with a total visible energy estimate of 4.6×10^{12} joules. This bolide explosion was observed by IMS stations in Hawaii, Alaska, California, Canada, and Germany. We use these two events to study the capabilities and limitations of source location procedures based on travel times and azimuth deviations that are derived from ray tracing formulations. A software algorithm has been developed to ingest accurate atmospheric profiles, which may be provided in near-real-time, use the tau-p method to compute the effective speed, or celerity, of specified infrasonic phases, and export these model results into any standard location algorithm, such as the Generic Locator (genloc) module within the Antelope software platform. This implementation is flexible as well as computationally efficient, and allows the exploitation of Center for Seismic Studies (CSS) (now Center for Monitoring Research) database structures and analysis tools.

OBJECTIVE

The aim of this work is to describe a ray-tracing algorithm for locating infrasonic sources, and to apply this algorithm to the determination of the position and origin time of two bolides detected by infrasound arrays in Hawaii and Alaska.

RESEARCH ACCOMPLISHED

Introduction

The tau-p method of Garcés *et al.* (1998, 2001, 2002) has been refined to clearly identify propagating infrasonic phases. Broadband infrasonic array measurements can be used to extract the amplitude, arrival time, apparent horizontal phase velocity, and azimuth of an arrival. All parameters can be estimated as a function of frequency using the PMCC method (Garcés and Hetzer, 2002). These detection parameters can be used to identify a phase, which is a prerequisite for estimating a source location. Given an atmospheric model, travel-time curves and azimuth deviations can be computed for each phase at any specified arrival azimuth. The apparent speed, or celerity, of a guided arrival is defined as the ratio of the range to the travel time for one or more multi-path bounces. Infrasonic phases identified to date are defined in Table 1, and are compatible with Brown's (1999) nomenclature and the IAVCEI list of propagating seismic phases.

Initial studies concentrated on an exact specification of the propagation path (Le Pichon *et al.*, 2002a,b; Liszka and Garcés, 2002), and these works were successful in cases when the range from the source to the receiver was not too large or along the dominant stratospheric wind direction. However, the detection of signals with high celerity propagating against the dominant stratospheric wind direction and the observation of apparent horizontal phase velocities lower than the speed of sound at the ground suggest that the interaction of infrasonic waves with atmospheric or topographical structures may scatter and diffract energy from elevated wave guides into the ground. We illustrate the critical issue of phase identification and the application of the location algorithm by using the bolide explosions of April 23, 2001, and August 25, 2000, as case studies. Because of its greater simplicity, we begin with an analysis of the 2001 bolide.

Event Selection and Array Detections of the April 23, 2001, Bolide

Infrared sensors aboard US Department of Defense (DOD) satellites detected the impact of a bolide on 23 April 2001 at 06:12:35 UTC (988006355 Epoch time). The bolide appeared to explode at an altitude of 28.5 km above the coordinates of 27.9 North and 133.89 West. The impact was simultaneously detected by space-based visible wavelength sensors operated by the US Department of Energy (DOE). The total energy in the visible band was 4.6×10^{12} joules. The location for the April 23 event determined by the optical systems is referred to as LO1. Since bolides often propagate at speeds of a few tens of kilometers per second, and there is no guarantee that the infrared detection coincided with the infrasonic signal generation, we postulate that the time of the LOI is more precise than the location of the detection.

The locations of the three nearest IMS arrays that detected the April 23 event are given in Table 2.1, and are shown in the upper panel of Figure 1. The upper panels of Figures 2-5 shows the PMCC (Garcés and Hetzer, 2002) detections for all three arrays. Comparison with the InfraTool detections for IS59 (Garcés *et al.*, 2001) shows that the first arrivals for PMCC are 226 seconds (4.4 minutes) earlier than the InfraTool first arrivals. This is an important result, as the first arrival time and the phase identification of that first arrival are essential to the location of infrasonic sources. Table 2.2 shows the maximum celerity values for select propagating phases. The list of Table 1 outlines all candidate phases, but for propagating ranges greater than a few thousand kilometers, it is difficult to sustain the *iw* phases and the *Iw*, *Is*, and *It* phases are not applicable. For long ranges, *is* phases are also found to be unstable, as the stratospheric winds can vary significantly along a meridian. However, the *it*, *itd*, and *isd* phases are found to exist for almost all azimuths and geographic locations. Only when an *is* phase exists does the *itd* phase disappear. For long ranges, the time contribution from the source height to the ground or the source height to the upper waveguide boundary is negligible, multiple bounces produce overlapping travel-time curves that begin to appear as a continuous curve, and shadow zones disappear. The *itd* and *isd* phases (Table 1) correspond to leaky wave guides that are suspended above the ground, but either scatter or diffract acoustic energy to the ground. Sources that explode at heights of ~30 km, such as the April 23 bolide, place acoustic energy in the middle of the low-velocity zone of the stratosphere, and thus efficiently trap energy in the stratospheric duct. This waveguide would be able to duct energy with minimal attenuation, and most first arrivals with high celerity may be attributed to *isd* phases. Due to the continuous appearance of travel-time curves and the further degradation of shadow zones by

24th Seismic Research Review – Nuclear Explosion Monitoring: Innovation and Integration

scattering and diffraction, we opt to use the celerity as the key propagation model output for the source location iteration.

Infrasonic Location Procedure for April 23 Event

From intersecting back azimuths, it is possible to produce a seed location for the source inversion procedure. However, as can be seen in Figure 1, the back azimuth location may be expected to be in error. An initial origin time can be obtained from the seed location by assuming a constant celerity of 0.3 km/s and computing the great circle paths to the source. Alternatively, if ground truth is known on an event, such as the epicentral location issued by the DoD release, the range of each station to the source and the expected azimuth of the incoming signal can be readily computed. Once an initial azimuth from source to receiver is determined, the tau-p method of Garcés *et al.* (1998, 2002) can be used to compute the celerity of each propagating phase. The lower panels of Figures 2-4 show the celerity computed at each array for the April 23 bolide using the Naval Research Laboratory's (NRL) SAGE atmospheric profiles that include accurate specifications of the troposphere and stratosphere (Garcés *et al.*, 2001). The estimated times of arrival of the first or second arrival at the station were used to compute the residuals from a grid search around the seed source location and origin time. Various locations were made assuming different phase identifications for both first and second arrivals (when present), but only two solutions (with the minimal residuals) are shown in Table 2.3. The first solution, LA_S1, assumes all first arrivals correspond to *isd* phases, and produced a very good match to the origin time provided by the satellite observation (LO1). Although in seismic location an 8-s time differential is unacceptable, when scaled to the total travel time of the signal, the percent error is small and comparable to the best seismic location accuracies (Table 2.4). The difference in the source location between LO1 and LA_S1 may be attributed to the high speed of the bolide and could correspond to a difference in where the peak sound and infrared energy are radiated. This result suggests that *isd* phases can be used to explain the arrival of signals in the upstream stratospheric direction, and the relatively higher frequency of the first arrivals observed in Figure 2 and 3 suggest that scattering is an important factor. A second solution, LA_S2, assumed that the first arrival at IS53 was an *isd* phase, the second arrival at IS57 was an *itd* phase, and the second arrival at IS59 was an *isd* phase. These phases were selected in an attempt to match the source location at the expense of the origin time. However, we favor the first solution because we believe the uncertainty in time (~10 s) may be less than the uncertainty in position for the satellite location LO1.

Infrasonic Location Procedure for the August 25, 2000, Event

The August 25, 2000, bolide, known as the Acapulco bolide, is more difficult to unravel. Table 3.1 shows the infrasonic observations for the Acapulco bolide. The arrival information for the stations in South America was derived from PMCC results (Le Pichon, personal communication, 2000). The lower panel of Figure 1 shows the station locations and back azimuths, again showing a poor azimuth fit of some of the stations to the actual source location. In general, it appears that the worst azimuth deviations occur in stations with extreme topography along the propagation path, specifically IS53 (Alaska) and IS08 (Bolivia). From the seed locations, azimuths from the stations to the source were estimated and the celerity computed at each station. Table 3.2 shows the maximum celerity for each phase. Figure 6 shows the PMCC detection at DLIAR, the closest station, and the change in detection azimuth with time. Following the same procedure as for the April 23 event, we computed locations for various permutations of phase identifications for the first and second arrival times. An attempt was also made to separate the detections into two events, one recorded by the US stations and another by the South American stations. However, two-station locations are inherently unstable, and even the solution using the three US stations was unstable because of the near parallel alignment of the DLIAR and IS53 propagation paths from the source. Three solutions are shown in Table 3.3. The first solution, LA_DL1, assumes all first arrivals are *isd* phases, and yielded a large error on the origin time estimate as well as in the time differentials for some of the stations (Table 3.4). The second solution, LA_DL2, assumed a combination of *it*, *itd* and *isd* phases (Table 3.5) and yielded a good fit to the origin time, although the time differentials per station are not as good as the April 23 solution. A source location west of the LO1 location is consistent with the DLIAR observations. Further work is needed to determine whether this event consists of a single bolide or more than one bolide arriving at different times, as suggested by the infrasound detections from IS25.

CONCLUSIONS AND RECOMMENDATIONS

Infrasonic estimates of the origin time and location of the April 23 event were performed using realistic atmospheric profiles and the tau-p method to estimate the celerity of propagating phases in the atmosphere. Arrivals corresponding to phases propagating in leaky stratospheric ducts produced the best fit to the origin time obtained from the satellite infrared detection. This existence of these leaky stratospheric ducts may explain how stratospheric

24th Seismic Research Review – Nuclear Explosion Monitoring: Innovation and Integration

phases can be observed along both the upstream and downstream dominant stratospheric wind directions. Further work is needed on how topography and perturbations in the atmosphere can scatter and diffract infrasonic energy into and out of elevated wave guides. The next generation of the tau-p software will address propagation in range-dependent environments.

REFERENCES

- Brown, D.J. (1999). Summary of infrasound source location meeting: San Diego, November 9-10, 1998, *Center for Monitoring Research*, Arlington, VA.
- Garcés, M, and C. Hetzer (2002). Evaluation of infrasonic detection algorithms. *This volume*.
- Garcés, M., D. Drob, and M. Picone (2002). A theoretical study of the effect of geomagnetic fluctuations and solar tides on the propagation of infrasonic waves in the atmosphere. *Geophys. J. International*, **148**, 77-87.
- Garcés, M, C. Hetzer, K. Lindquist, and R. Hansen, J. Olson, C. Wilson, D. Drob, M. Picone, (2001). Infrasonic location of the April 23, 2001, Bolide event. *23rd Annual DTRA/NNSA Seismic Research Review*, Jackson Hole, 1-5 October 2001.
- Garcés, M, D. Drob, M. Picone, K. Lindquist, and R. Hansen (2000). Characterization Of Infrasonic Waves Observed In Hawaii During Summer, *22nd Seismic Research Symposium: Planning for Verification of and Compliance with The Comprehensive Nuclear-Test-Ban Treaty*, New Orleans.
- Garcés, M. A., R. A. Hansen, and K. Lindquist (1998). Travel times for infrasonic waves propagating in a stratified atmosphere, *Geophys. J. International*, **135**, 255-263.
- Le Pichon, A. M. Garcés, E. Blanc, M. Barthélémy, D. Drob (2002). Acoustic propagation and atmosphere characteristics derived from infrasonic waves generated by the Concorde. *J. Acoust. Soc. Am.*, **111**, 629-641.
- Le Pichon, A., J. Guilbert, A. Vega, and M. Garcés (2002), Ground-coupled air-waves and diffracted infrasound from the Arequipa earthquake of June 23, 2001, *Geophysical Research Letters* (in press).
- Liszka, L., and M. Garcés (2002), Infrasonic Observations of the Hekla Eruption of February 26, 2000. *Journal of Low Frequency Sound* (in press).
- Kulichkov, S. N. (1998). On problems of infrasonic monitoring of small energy explosions, *Proceedings of the Informal Workshop on Infrasound*, Bruyeres-Le-Chatel, France.

Table 1. Preliminary phase identification nomenclature for long-range infrasonic propagation

| Phase ID | Description | Typical celerity of first arrival, m/s |
|------------|--|--|
| iw | Guided wave propagating between the tropopause and the ground. | 330-340 |
| is | Guided wave propagating between the stratopause and the ground. | 310-330 |
| isd | Guided wave propagating in elevated waveguide between stratopause and the troposphere, and diffracted or scattered to the ground. May have higher frequency. | 310-330 |
| it | Guided wave propagating between the lower thermosphere and the ground. | 280-300 |
| itd | Guided wave propagating in elevated waveguide between the lower thermosphere and the troposphere, and diffracted or scattered to the ground. | 280-300 |
| It, Is, Iw | Direct arrival from the source to the receiver. May have high apparent phase velocity | N/A |

Table 2.1. First arrival observations of April 23, 2001, bolide by three nearest IMS infrasound stations

| Station | Lat (N) | Lon (E) | Speed (m/s) | Azimuth | ETA (epoch) |
|-------------|---------|---------|-------------|---------|-------------|
| IS53 | 64.87 | -147.84 | 322 | 150.6 | 988020690 |
| IS57 | 33.6 | -116.5 | 349 | 256.1 | 988012060 |
| IS59 | 19.59 | -155.9 | 348 | 63.6 | 988013790 |

Table 2.2. Predicted first arrival celerity (km/s) for select phases: April 23, 2001

| | it | itd | isd |
|-------------|-------|-------|-------|
| IS53 | 0.268 | 0.284 | 0.292 |
| IS57 | 0.278 | 0.292 | 0.328 |
| IS59 | 0.284 | 0.3 | 0.311 |

Table 2.3. Source location and errors relative to satellite location (LO1): April 23, 2001

| Source | Lat (N) | Lon (E) | Origin Time (Epoch) | Lat error (deg) | Lon error (deg) | Time error (s) |
|--------------|---------|---------|---------------------|-----------------|-----------------|----------------|
| LO1 | 27.9 | -133.89 | 988006355 | 0 | 0 | 0 |
| LA_S1 | 28.07 | -135.09 | 988006347 | 0.17 | -1.2 | -8 |
| LA_S2 | 27.79 | -133.42 | 988006145 | -0.11 | 0.47 | -210 |

Table 2.4. Phase selection and time error for LA_S1 solution: April 23, 2001
 PA = predicted arrival; ETA = first arrival time; OT = origin time

| Station | Selected Phase | Range to LA_S1 | X/T (km/s) | Predicted arrival | Time Error /Travel Time | PA-ETA | PA-OT | Ratio (%) |
|-------------|----------------|----------------|------------|-------------------|-------------------------|--------|-------|-----------|
| IS53 | isd | 4191 | 0.292 | 988020700 | -0.06% | 10 | 14353 | 0.07 |
| IS57 | isd | 1877 | 0.328 | 988012070 | -0.14% | 10 | 5723 | 0.17 |
| IS59 | isd | 2313 | 0.311 | 988013784 | -0.11% | -6 | 7437 | 0.08 |

Table 3.1. First arrival observations of August 25, 2000, bolide by infrasound stations.

| Station | Lat (N) | Lon (E) | Speed (m/s) | Azimuth | ETA (epoch) |
|---------|---------|---------|-------------|---------|-------------|
| IS08 | -16.3 | -68.1 | 340 | 298 | 967184490 |
| IS25 | 5.2 | -52.7 | 344 | 283 | 967187730 |
| IS53 | 64.87 | -147.84 | 355 | 144 | 967187230 |
| IS59 | 19.59 | -155.9 | 346 | 88 | 967182900 |
| DLIAR | 35.87 | -106.33 | 360 | 180 | 967173900 |

Table 3.2. Predicted first arrival celerity (km/s) for select phases: August 25, 2000

| | it | itd | isd |
|-------|-------|-------|-------|
| IS08 | 0.289 | | 0.298 |
| IS25 | 0.263 | 0.285 | 0.29 |
| IS53 | 0.292 | 0.303 | 0.31 |
| IS59 | 0.281 | 0.297 | 0.308 |
| DLIAR | 0.278 | | 0.309 |

Table 3.3. Source location and errors relative to satellite location (LO1): August 25, 2000

| Source | Lat (N) | Lon (E) | Origin Time (Epoch) | Lat error (deg) | Lon error (deg) | Time error (s) |
|--------|---------|---------|---------------------|-----------------|-----------------|----------------|
| LO1 | 14.45 | -106.13 | 967165945 | 0 | 0 | 0 |
| LA_DL1 | 13.68 | -108.21 | 967166247 | -0.77 | -2.08 | 302 |
| LA_DL2 | 13.37 | -107.74 | 967165950 | -1.08 | -1.61 | 5 |

Table 3.4. First arrival phase selection and time error for LA_DL1 solution: August 25, 2000

| Station | Selected Phase | Range to LA_DL1 | X/T (km/s) | Predicted Arrival | Time Error / Travel Time | PA-ETA | PA-OT | Ratio (%) |
|---------|----------------|-----------------|------------|-------------------|--------------------------|--------|-------|-----------|
| IS08 | isd | 5513 | 0.298 | 967184747 | 1.63% | 257 | 18500 | 1.39 |
| IS25 | isd | 6149 | 0.290 | 967187450 | 1.39% | -280 | 21203 | -1.32 |
| IS53 | isd | 6432 | 0.310 | 967186995 | 1.42% | -235 | 20748 | -1.13 |
| IS59 | isd | 5110 | 0.308 | 967182838 | 1.78% | -62 | 16591 | -0.37 |
| DLIAR | isd | 2464 | 0.309 | 967174221 | 3.80% | 321 | 7974 | 4.03 |

Table 3.5. First arrival phase selection and time error for LA_DL2 solution: August 25, 2000

| Station | Selected Phase | Range to LA_DL2 | X/T (km/s) | Predicted Arrival (PA) | Time error / Travel time | PA-ETA | PA-OT | Ratio (%) |
|---------|----------------|-----------------|------------|------------------------|--------------------------|--------|-------|-----------|
| IS08 | it | 5452 | 0.289 | 967184815 | 0.03% | 325 | 18865 | 1.72 |
| IS25 | itd | 6096 | 0.285 | 967187339 | 0.02% | -391 | 21389 | -1.83 |
| IS53 | itd | 6481 | 0.303 | 967187339 | 0.02% | 109 | 21389 | 0.51 |
| IS59 | isd | 5168 | 0.308 | 967182729 | 0.03% | -171 | 16779 | -1.02 |
| DLIAR | isd | 2495 | 0.309 | 967174024 | 0.06% | 124 | 8074 | 1.54 |

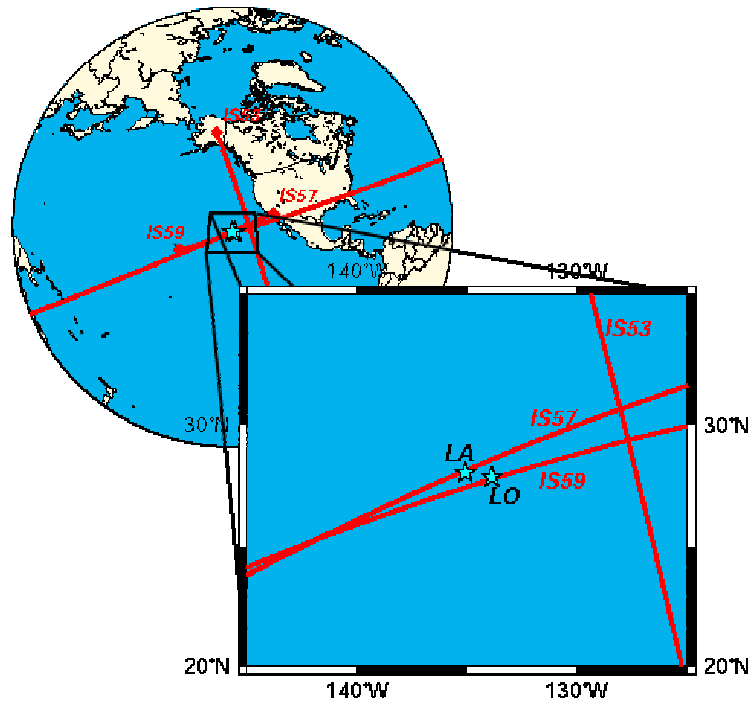


Figure 1. Satellite (LO) and infrasonic (LA_S1) location for the April 23, 2001, bolide. The observed arrival azimuths at infrasound arrays IS53, IS57, and IS59 are shown as red lines.

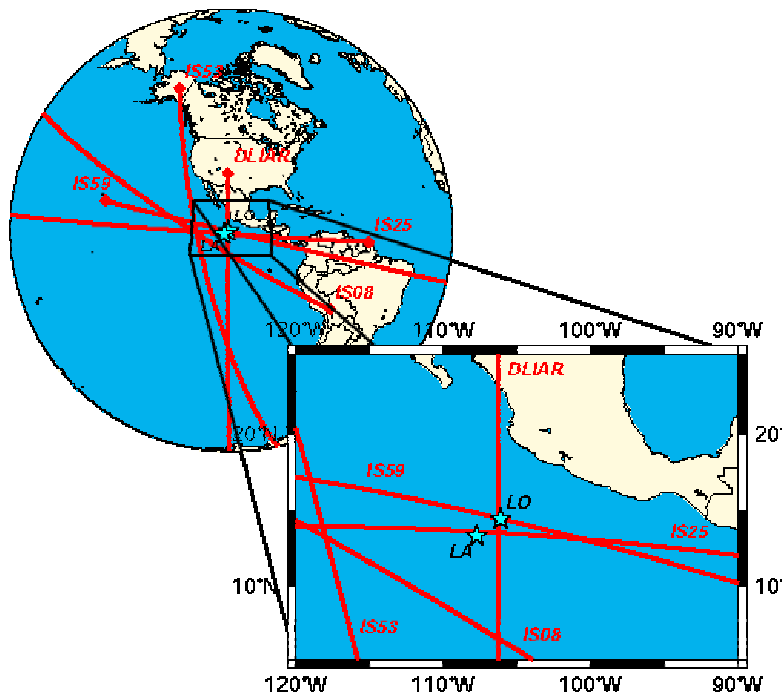


Figure 2. Satellite (LO) and infrasonic (LA_DL2) location for the Acapulco bolide. The observed arrival azimuths at infrasound arrays IS08, IS25, IS53, DLIAR, and IS59 are shown as red lines.

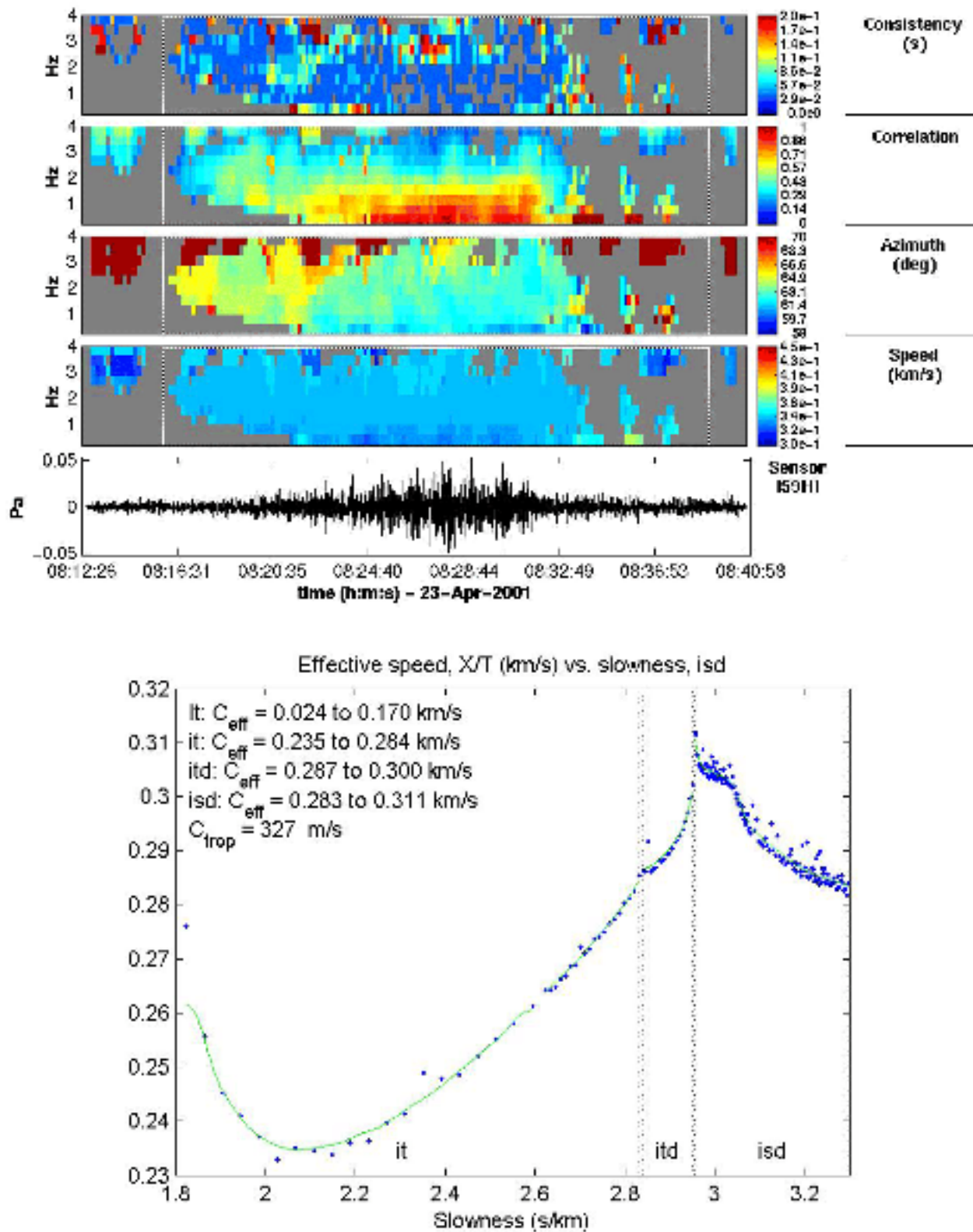


Figure 3. Detection and predicted celerity at IS59, Hawaii, for April 23, 2001, bolide.

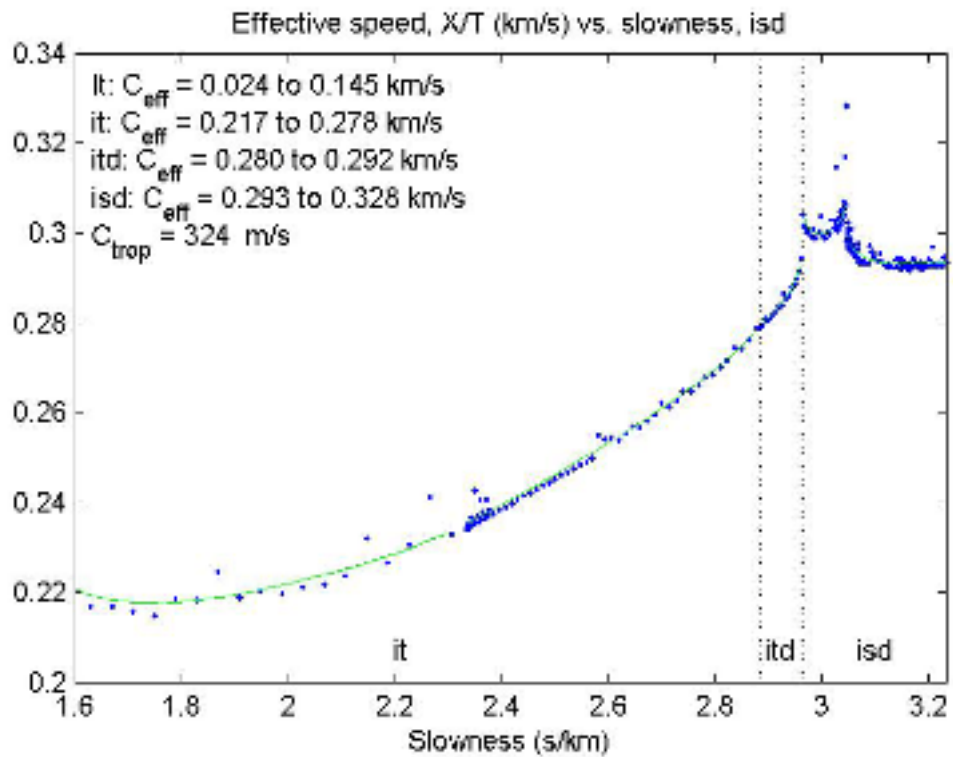
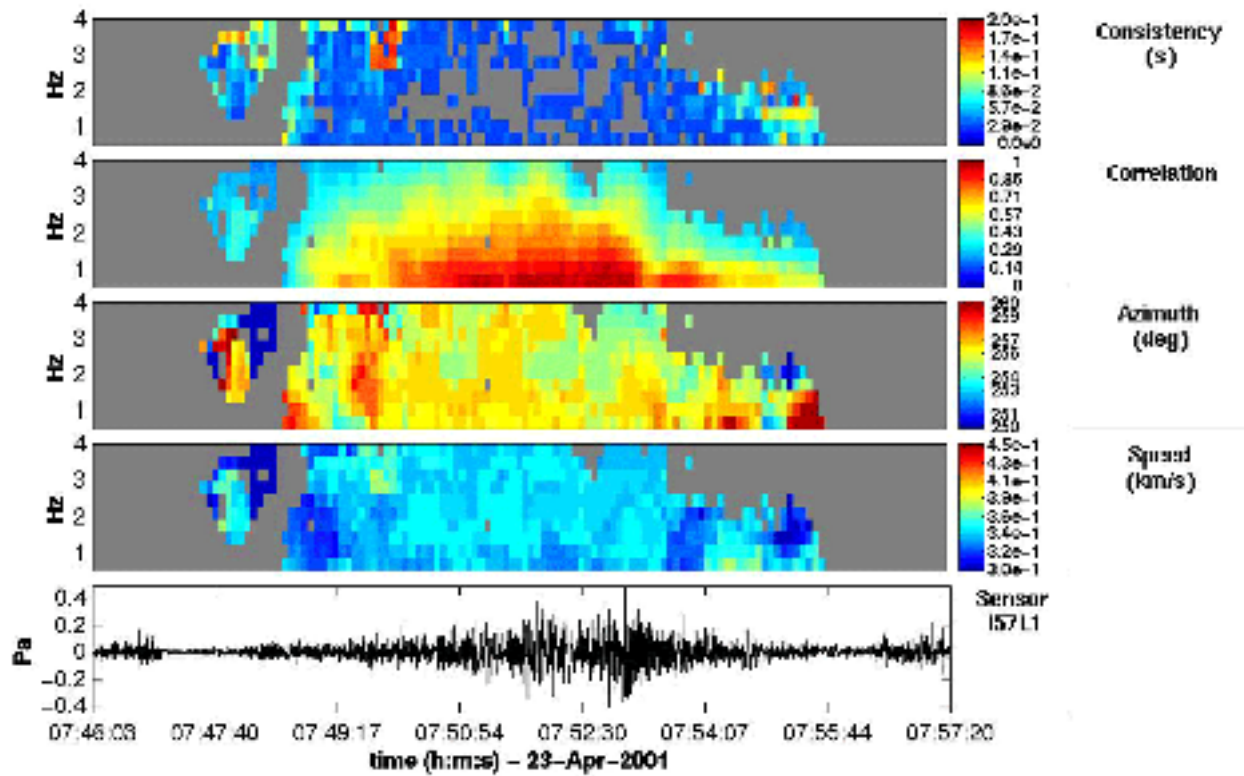


Figure 4. Detection and predicted celerity at IS7, Piñon Flats, for April 23, 2001, bolide.

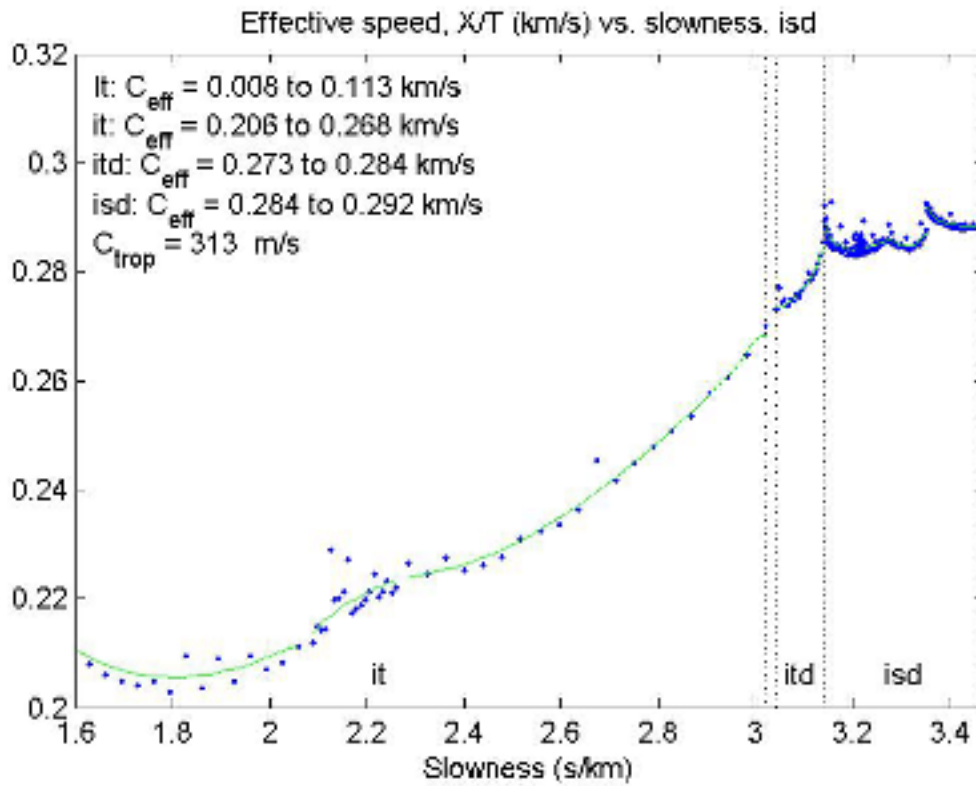
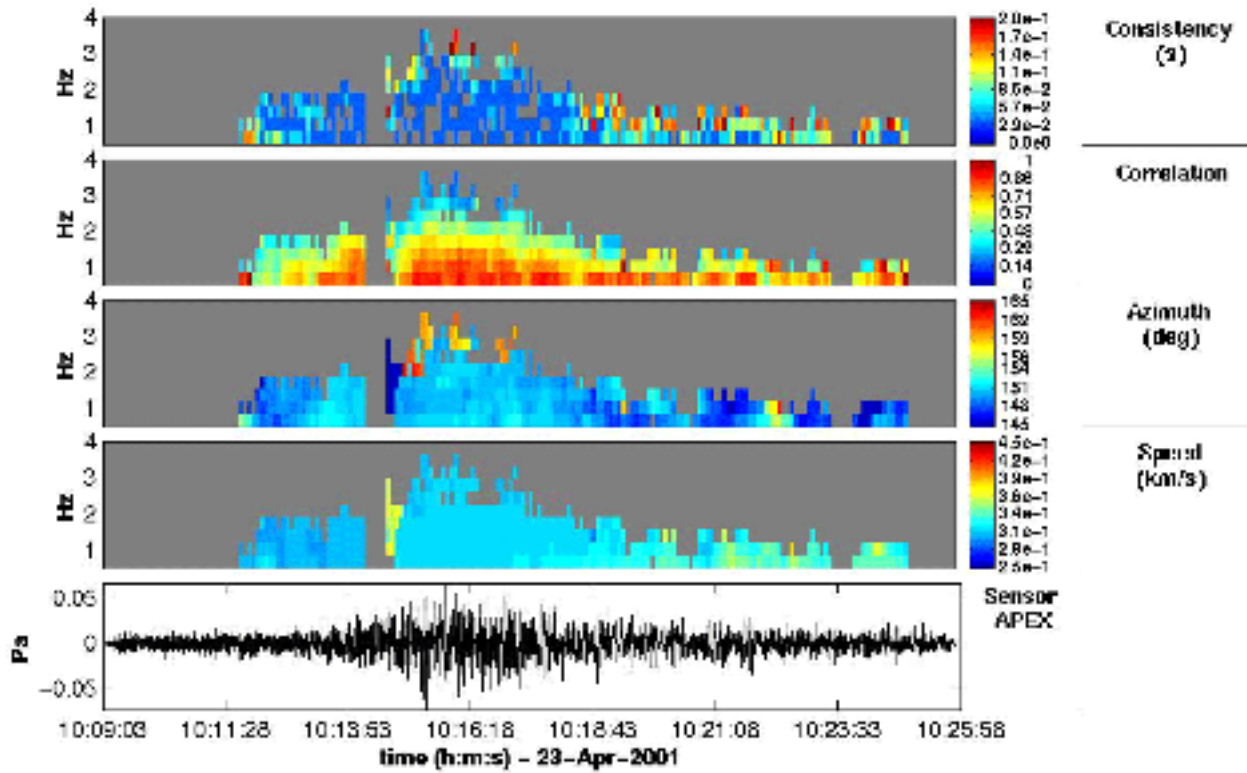


Figure 5. Detection and predicted celerity at IS53, Fairbanks, Alaska, for April 23, 2001, bolide.

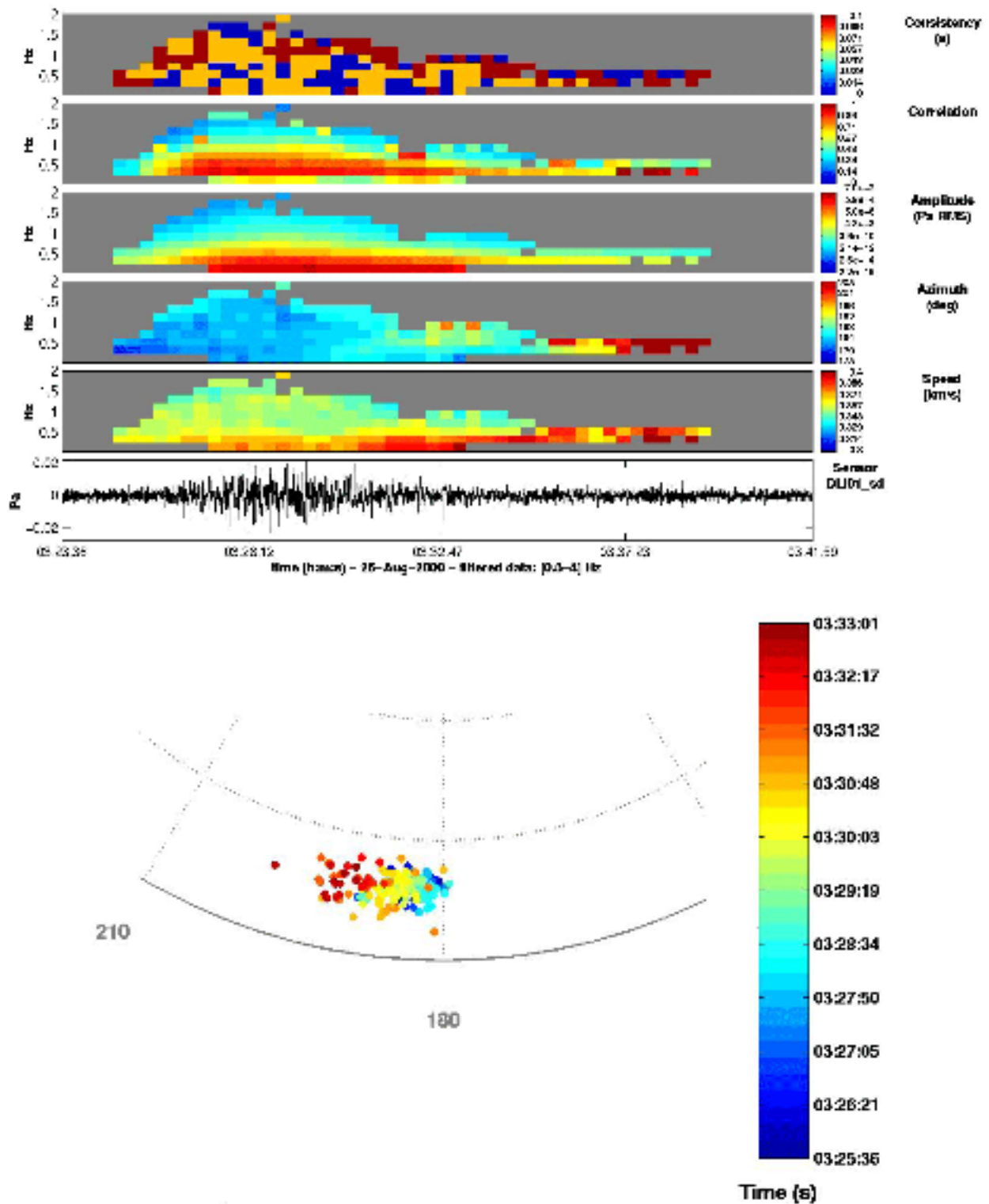


Figure 6. Detections and azimuth changes as a function of time observed at DLIAR, New Mexico, for the Acapulco bolide.